Equivalent Viscous Damping for the Displacement-Based Seismic Assessment of Infilled RC Frames

L. Landi, P.P. Diotallevi & A. Tardini
Department of Civil, Environmental and Materials Engineering - DICAM, University of Bologna, Bologna, Italy

SUMMARY:
According to the displacement-based approach, in the seismic assessment of existing buildings it is required the definition of the equivalent viscous damping of the structure under study. As the hysteretic damping represents a measure of the dissipative capacity of structures, it is expected that it is larger for RC frames with masonry infills than for bare frames. At the date, the assessment procedure proposed within the displacement-based approach concerns only bare frame. The objective of this study was to extend the procedure to infilled RC frames by defining a ductility-damping law valid for this kind of frames. In order to obtain the mentioned relationship, several nonlinear dynamic analyses were carried out by applying different ground motions to single storey-single bay infilled frames. The effectiveness of the proposed ductility-damping law was then verified by comparing the displacement demand calculated with the assessment procedure with that obtained from nonlinear dynamic analyses.

Keywords: Displacement-Based Assessment; Equivalent Viscous Damping; Infilled Frames

1. INTRODUCTION

The Displacement-Based Design (DBD) (Priestley et al., 2007) is based on the schematization of a general structure as a linear single-degree of freedom (SDOF) system characterized by equivalent height and mass. The equivalent system is defined in order to represent the response of the structure at peak displacement rather than the initial elastic behaviour. This SDOF structure is characterized by the secant stiffness at maximum displacement and by a level of equivalent viscous damping. The same approach is proposed for the seismic assessment of existing structures. The seismic assessment allows determining the displacement demand that has to be compared with the displacement capacity. The displacement demand is determined by an iterative procedure in which it is necessary to calculate the equivalent damping of the structure. To this purpose it is possible to use some ductility-damping laws proposed in literature depending on the structural typology (Iwan and Gates, 1979; Judi et al. 2001). The equivalent damping is the sum of two contributions: the inherent damping, normally taken as 5% for all types of structures, and the hysteretic damping, which depends on the dissipative capacity of the different structures. In case of infilled frames the common practice does not consider the presence of infill and accounts for only the RC frame. However it is known that the masonry infill could produce significant effects on the seismic response of buildings. In particular the infill could determine positive or negative effects. In the first case it can increase the strength and the dissipative capacity of the structure, in the second case it can produce unexpected distributions of forces and consequent local phenomena of collapse. Considering only bare frame may lead to underestimating the dissipative capacity of the structure and the hysteretic damping. As the hysteretic damping represents a measure of the dissipative capacity of structures in the inelastic range, it is expected that it is larger for RC frames with masonry infills than for bare frames. This difference will be larger for little values of ductility demand. On the contrary, due to the deterioration of the infills the values of hysteretic damping of infilled and bare frames tend to be similar with the increase of ductility demand. The objective of this study was to evaluate the equivalent damping of infilled frames in order to define a ductility-damping law valid for this kind of structures.

2. PROCEDURE FOR THE EVALUATION OF THE EQUIVALNET DAMPING

As previously mentioned, various ductility-damping law were proposed in literature depending on the type of examined structure. In particular the following relationship was proposed for the design of RC bare frames (Priestley et al., 2007):

$$\xi_e = 0.05 + 0.565\left(\frac{\mu - 1}{\mu\pi}\right) \tag{2.1}$$

where μ represents the structure ductility demand. The aim of the present study was to define a relationship valid for infilled frame similar to Eqn. 2.1. In order to determine the equivalent damping several nonlinear dynamic analyses were carried out using different ground motions and considering single storey-single bay frames. The analyses were repeated for bare and infilled frames in order to compare the two responses. The adopted procedure can be synthesized in the following steps:

1. Apply a ground motion to the structure and determine the response in terms of force-displacement diagram.
2. Identify the maximum displacement (δ_{max}) caused by the ground motion and the relative ductility μ, calculated with reference to the yield displacement.
3. Determine the secant stiffness K_{sec} corresponding to the maximum displacement (Fig. 2.1a) and then calculate the relative period T_{sec}.
4. Identify the reduced displacement spectrum relative to the considered earthquake record which intercepts the point (T_{sec}, δ_{max}) (Fig. 2.1b) and determine the corresponding damping. In this way a couple of values ductility-damping valid for this single examined case is obtained.
5. Steps 1-4 are repeated using the same earthquake record scaled to different values of intensity. In this way some couples μ-ξ are obtained.
6. The entire procedure is repeated using different ground motions.
7. All the results are interpolated in order to build the average curves.

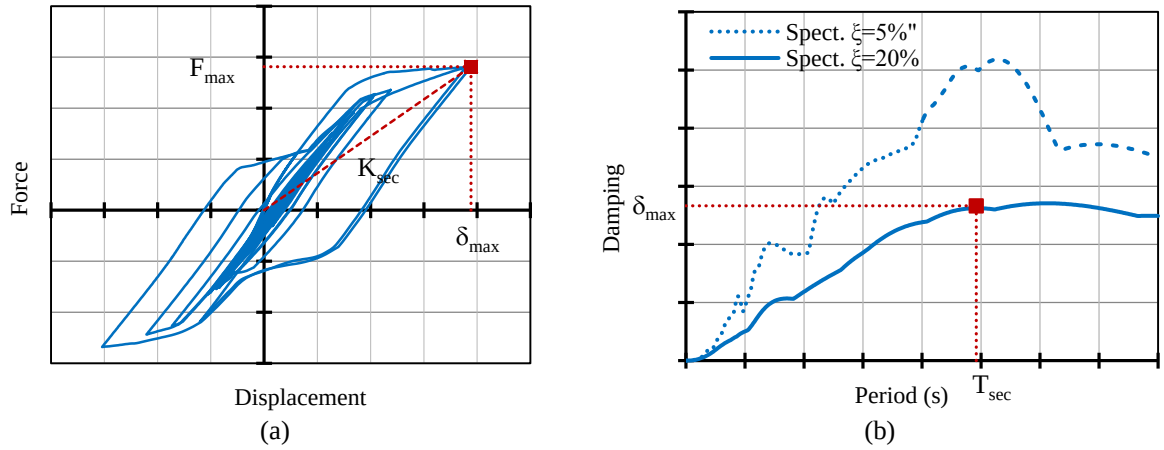

Figure 2.1. Graphic representation of the most important steps in the evaluation of the equivalent damping: determination of the secant stiffness (a) and of the reduced displacement spectrum (b)

This analysis was performed for values of ductility demand of the bare frame smaller than 5. This is the range of values in which the infill modifies the seismic structural response. In order to calculate the ductility, the yield displacement considered was the one of the bare frame. This displacement was calculated from the expression of the yield drift proposed in literature (Priestley et al., 2007):

$$\theta_y = 0{,}5\varepsilon_y \frac{L_b}{h_b} \tag{2.2}$$

where ε_y is the steel yield strain while L_b and h_b are respectively the length and the height of the beam. It should be noticed that also the ductility of the infilled frame was calculated with reference to the yield displacement of the bare frame. This choice is motivated by two reasons. The first is that the determination of the yield displacement for infilled frames is more doubtful. The second reason is related to the possibility of obtaining a ductility-damping law to be used directly with the characteristics of the bare frame, even in the case in which the infills are present. If it is possible to refer directly to the yield displacement of the bare frame, it is not necessary to know the one of the infilled frame. Considering the yield displacement of the infilled frame would only change the scale of value. Once the maximum displacement was determined for each ground motion, two cases were examined, depending on the secant stiffness used to calculate the period. In the first case the secant stiffness considered was the one related to the monotonic force-displacement response of the bare frame (K_{bare}). In the second case the secant stiffness considered was the one related to the monotonic force-displacement response of the infilled frame (K_{inf}). This distinction was examined with the purpose to evaluate whether it is necessary to know the detailed response of the infilled frame or it is enough to know the one of the bare frame. In Fig. 2.2 it is possible to see the two different stiffnesses related to the force-displacement response of the bare and infilled frame.

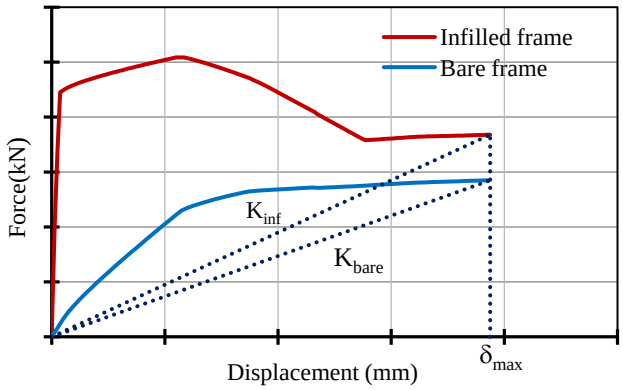

Figure 2.2. Secant stiffnesses related to the bare and infilled frame response

3. STRUCTURES UNDER STUDY

The described procedure was applied to three different single storey-single bay RC frames (frame 1, frame 2 and frame 3). Each one was considered with and without infills. All the frames have the same geometrical dimensions (Fig. 3.1a) and steel amounts. As a consequence they show the same lateral strength (Fig. 3.1b). They have also different masses and therefore different elastic periods, as shown in Table 3.1. The assumed mechanical properties of materials are: concrete cylinder strength f_{ck} equal to 28 Mpa and steel yield strength f_{yk} equal to 450 Mpa. The adopted dimensions of beams are: width equal to 300 mm and depth equal to 500 mm. The adopted dimensions of columns are: width and depth equal to 300 mm. The considered infills are masonry panels with thickness of 15 cm, compressive strength of 4.1 N/mm^2 and shear strength of 0.3 N/mm^2.

Table 3.1 Elastic periods of the examined frames

	T elastic (s)
Frame 1	0.35
Frame 2	0.5
Frame 3	1

An important factor which characterizes the behaviour of an infilled frame is the ratio between the shear strength of the masonry and the one of the frame. In the model of the infilled frame proposed by Al-Chaar (2002), which was adopted in this study, this ratio influences the determination of the ultimate displacement of the infill. In the examined cases the lateral shear strength of the RC frame resulted equal to 140 kN while the shear strength of the infill resulted equal to 211 kN. Therefore a

value of about 1.5 was derived for the aforementioned ratio. Fig. 3.1 shows the base shear-displacement curves of the bare and infilled frames.

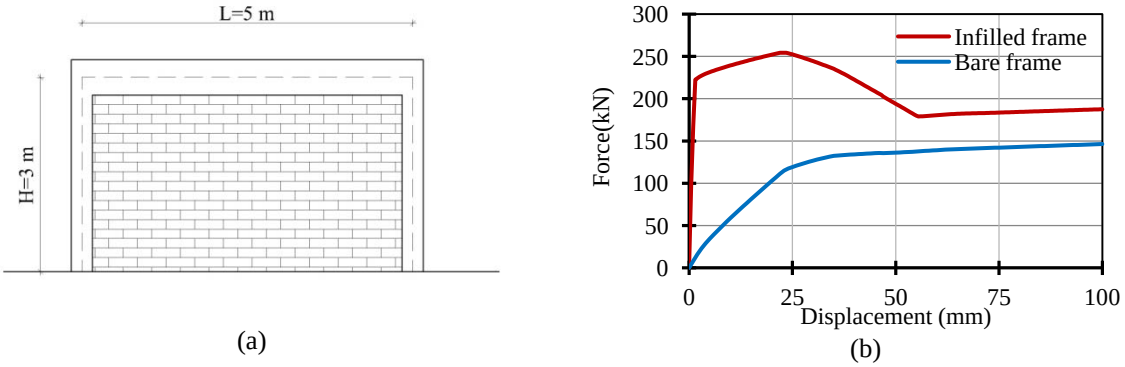

Figure 3.1. Geometrical configuration of the single storey-single bay frames (a) and force displacement response of the bare and infilled frames (b)

4. NONLINEAR MODEL AND PERFORMED ANALYSES

The nonlinear analyses were carried out in order to assess the performance of the structures under study. The OpenSees software (McKenna and Fenves, 2005) was used for the nonlinear analyses. This computer program allows studying the structure with distributed plasticity finite elements characterized by a fibre modelling of the control sections. The elements of the examined structures were modelled with a single finite element for each beam or column. For each element 5 control sections were adopted. A bilinear stress-strain relationship with hardening ratio equal to 0.005 was assumed for the steel fibres. A constitutive law, which includes the effect of confinement due to stirrup and the stiffness degradation due to cyclic loading, was considered for the concrete. Different types of behaviour were adopted for the cover concrete and the concrete core: in the first case the effect of confinement was neglected, in the second case it was included according to the model proposed by Mander et al. (1988). The infills were modelled by replacing the panel with a system of two equivalent struts. Each masonry strut was considered to be effective only in compression. The width and the strength of the strut were determined according to the model proposed by Al-Chaar (2002). The constitutive law assigned to the strut accounts for the degradation of stiffness and strength typical of the masonry (Fig. 4.1). The response for cyclic loading was studied as suggested by Cavaleri et al. (2005). A first calibration was carried out to determine the slope of the post peak branch, the residual strength and the loading and unloading branches. The calibration was performed by comparison with some experimental results available in the literature. The characteristics of the adopted model and the calibration are detailed in (Landi et al., 2012).

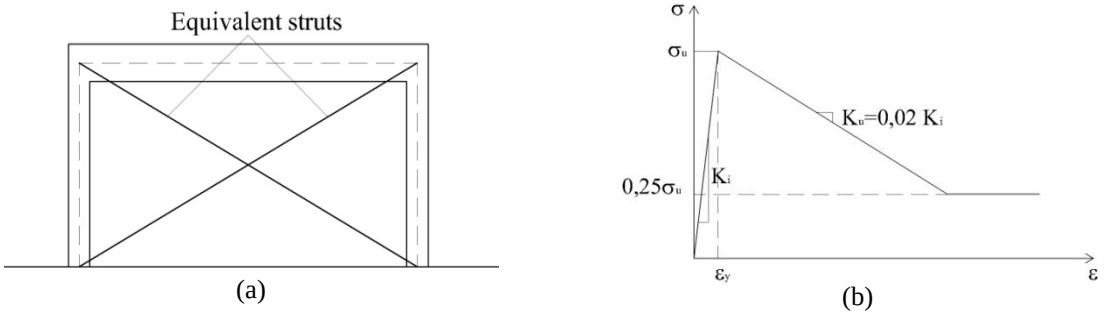

Figure 4.1. Equivalent diagonal struts (a) and stress-strain relationship assigned to the struts (b)

The nonlinear dynamic analyses were carried out using 2 sets of accelerograms (Set_1, Set_2). The first group consists of 7 accelerograms, including four recorded and three artificial ground motions. The second group consists of 5 recorded accelerograms. Both groups of ground motions have an

average displacement spectrum consistent with type 1 Eurocode 8 design spectrum. The displacement spectra related to the two sets of accelerograms are illustrated in Fig. 4.2. These accelerograms were applied with different intensity values in order to obtain values of ductility demand up to 5.

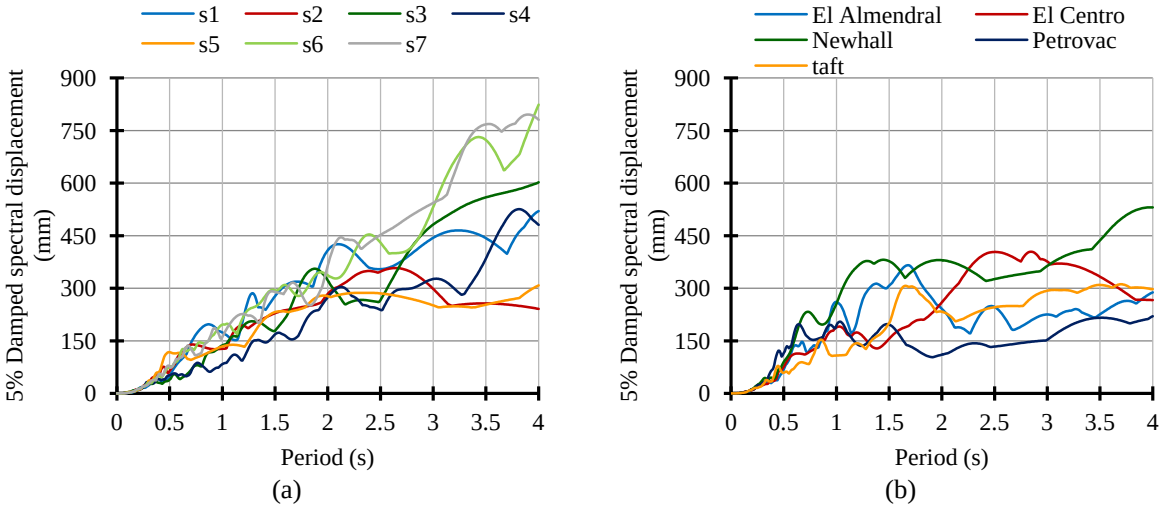

Figure 4.2. Displacement spectra of the selected ground motions scaled to PGA=0.5 g: Set_ 1(a) and Set_ 2 (b)

5. RESULTS OF THE ANALYSES

Each single nonlinear dynamic analysis provided a value of ductility demand and of equivalent damping and therefore a point in the ductility-damping diagram. All the analyses led to a series of points. From these points it was possible to construct the average curves that are shown in the following graphs with a red dotted line for each examined structure (Fig. 5.1, Fig. 5.2, Fig. 5.3). An hyperbolic ductility damping law according to the following expression, consistent with Eqn. 2.1, was determined in order to best approximate the average results :

$$\xi_{hyst} = C\left(\frac{\mu - \alpha}{\mu\pi}\right) \tag{5.1}$$

In the Eqn.5.1 C and α represent two coefficients that have to be determined. In particular α is the intersection point of the curve with the horizontal axis corresponding to hysteretic damping equal to 0, and C/π is the damping value for ductility tending to infinity. This type of relationship was originally proposed by the study of Dwairi et al. (2007). The determined hyperbolic curve is the ductility-damping law that was searched and is represented in the graphs by a continuous green line. Initially the average curve was separately built for the two groups of accelerograms (Fig. 5.1, Fig. 5.2). However the aim was to obtain a generic curve, so the overall average curve was determined by the same method, taking into account the results of both groups of accelerograms. The overall average curves are shown in Fig. 5.3. Each curve reproduces the results of all the three examined structures (Frame 1, 2, 3). The results regarding the infilled frame are illustrated by distinguishing the case in which the secant stiffness of the bare frame was considered in the procedure from the case in which the secant stiffness of the infilled frame was used. The two cases led to different values of damping. When the stiffness of the infilled frame was considered, the analysis was extended to ductility values less than 1. The infilled frame, in fact, dissipated also for these values of ductility and therefore it had a certain damping. However it was meaningful to assess this damping only by considering the stiffness of the infilled frame because in several analyses with the stiffness of the bare frame the values of damping resulted larger than 1 for low values of ductility. When considering the stiffness of the infilled frame the average curve was constructed using two different methods: the first (A) was the same used for the other cases and led to a hyperbolic curve valid for values of ductility larger than 1; the second method (B) consisted in finding a hyperbolic curve passing through the point α: this

parameter was calculated as the ratio between the yield displacement of the infilled frame and that of the bare frame.

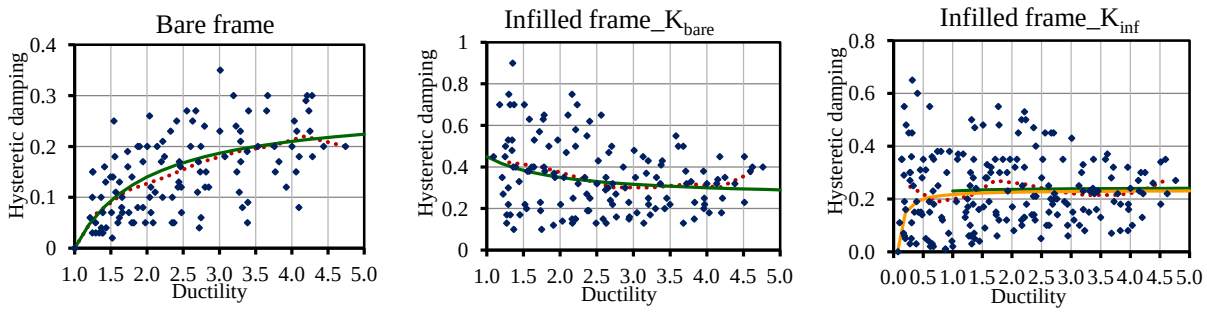

Figure 5.1. Ductility-damping values obtained from the analyses and average curves for the Set_1

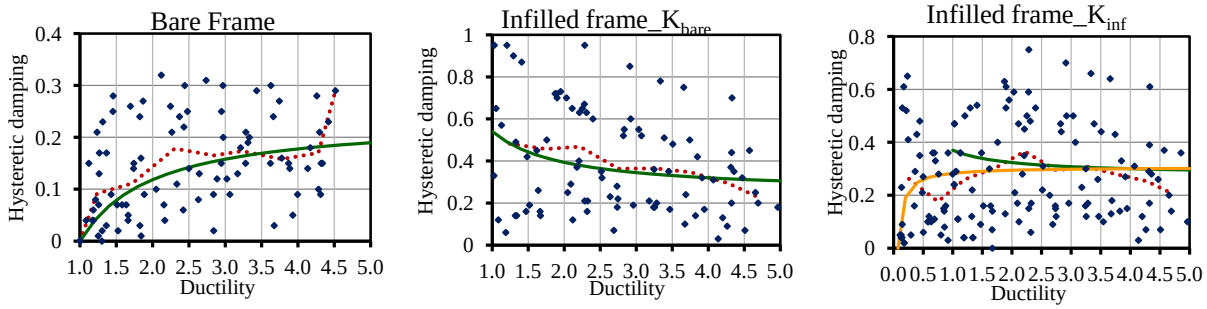

Figure 5.2. Ductility-damping values obtained from the analyses and average curves for the Set_2

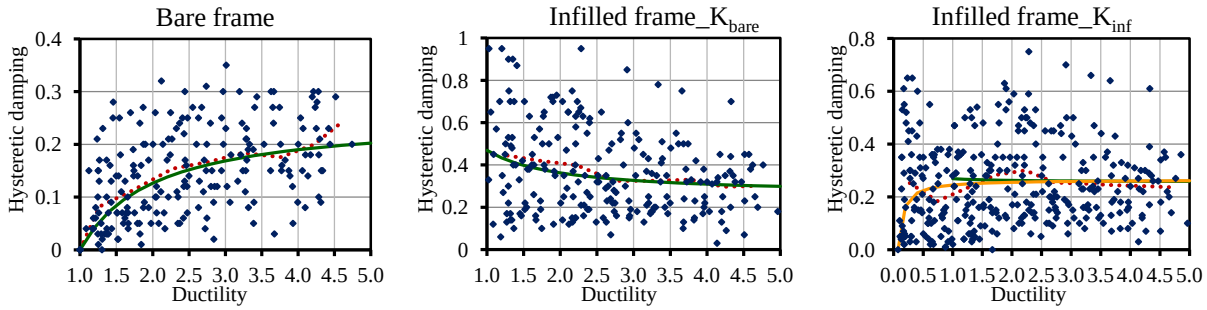

Figure 5.3. Ductility-damping values obtained from the analyses and average curves for all ground motions

The analytical expression is given for the overall average curves shown in Fig. 5.3. The following relationship was derived for the bare frame:

$$\xi_{hyst} = 0{,}794 \cdot \frac{\mu - 1}{\mu\pi} \tag{5.2}$$

The following relationship was obtained for the infilled frame, considering in the procedure the stiffness of the bare frame (K_{bare}):

$$\xi_{hyst} = 0{,}804 \cdot \frac{\mu + 0{,}83}{\mu\pi} \tag{5.3}$$

The following relationship was obtained for the infilled frame, considering in the procedure the stiffness of the infilled frame (K_{inf}) and using the methods A and B:

$$\xi_{hyst} = 0{,}804 \cdot \frac{\mu+0{,}05}{\mu\pi}, \quad \mu \geq 1, \text{ method A} \tag{5.4}$$

$$\xi_{hyst} = 0{,}83 \cdot \frac{\mu - 0{,}07}{\mu\pi}, \qquad \mu \geq 0 \text{ , method B} \tag{5.5}$$

Obviously the derived ductility-damping curves are affected by the characteristics of the examined structures and by the adopted accelerograms. The Fig. 5.4 shows the curves obtained for the bare frame compared with the one determined according to the relationship proposed in literature (Eqn. 2.1). In this figure it could be observed that the obtained curves are characterized by larger ordinates than the one of Eqn. 2.1; this fact is likely due to the number of examined cases. The curve of Eqn. 2.1, in fact, has been found considering a larger number of frames, subjected to hundred of accelerograms. Therefore the analysis of a larger series could give results more similar to Eqn. 2.1.

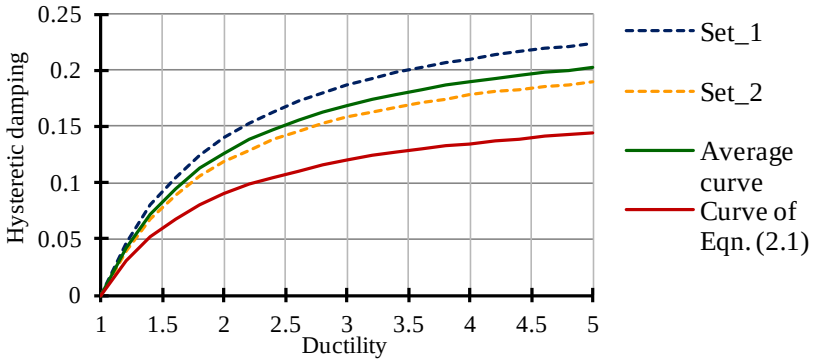

Figure 5.4. Average curves relative to the bare frame compared with the theoretical curve of Eqn. 2.1

With regard to the infilled frame the average curves obtained from the analyses are shown in Fig. 5.5. Firstly we can note that, using the stiffness of the bare frame, the hysteretic damping resulted greater than the one obtained with the stiffness of the infilled frame. The dynamic analyses carried out were the same in the two cases. The only difference was the secant stiffness that was used in calculating the period. With the same displacement but using a larger stiffness, like the one of the infilled frame, a shorter period was obtained. In this way the displacement spectrum passing through the new identified point (T_{sec}, δ_{max}) corresponded to a lower damping. It should be observed that the use of these two different stiffnesses does not lead to different estimates of the seismic response. If the Displacement Based (DB) assessment procedure is applied using the two different stiffnesses and then the two relative values of damping, the same values of displacement demand are obtained. From Fig. 5.5 it is possible to notice that the difference between the two cases decreases for increasing values of ductility. This happens because with the increase of ductility the contribution of the infill decreases and the two stiffnesses tend to coincide. Instead, for small values of ductility, for example smaller than 2, the difference between the two cases is significant. For these values of ductility, considering the stiffness of the bare frame (Fig. 5.5a) the obtained values of damping are very high because it is great the difference between the response of the infilled frame and that of the bare frame. In Fig. 5.5b, where the stiffness of the infilled frame is considered, it is possible to observe that the average curves obtained with the two methods A and B are very similar for values of ductility larger than 1.

Finally in Fig. 5.6 the overall average curves for the examined structures and for the considered cases are compared. It could be noticed that for high values of ductility the curves of the hysteretic damping of the bare and infilled frames tend to converge, because the contribution of the infill tend to be erased. Moreover, for ductility values greater than 2 the curves calculated with the stiffness of the bare or infilled frame are only slightly different, showing that in this case the knowledge of the stiffness of the infilled frame is not necessary. At last for ductility values lower than 2 it is necessary to know the stiffness of the infilled frame in order to calculate a reliable damping factor.

We could try to find a general relationship for the infilled frame using the coefficient C obtained for the bare frame and the coefficient α from Eqn. 5.5. In this way the ductility-damping law would be conservative because it would determine a lower value of damping than the one determined from the

analyses of this study, even taking into account the increase in damping for small ductility due to the presence of the infill.

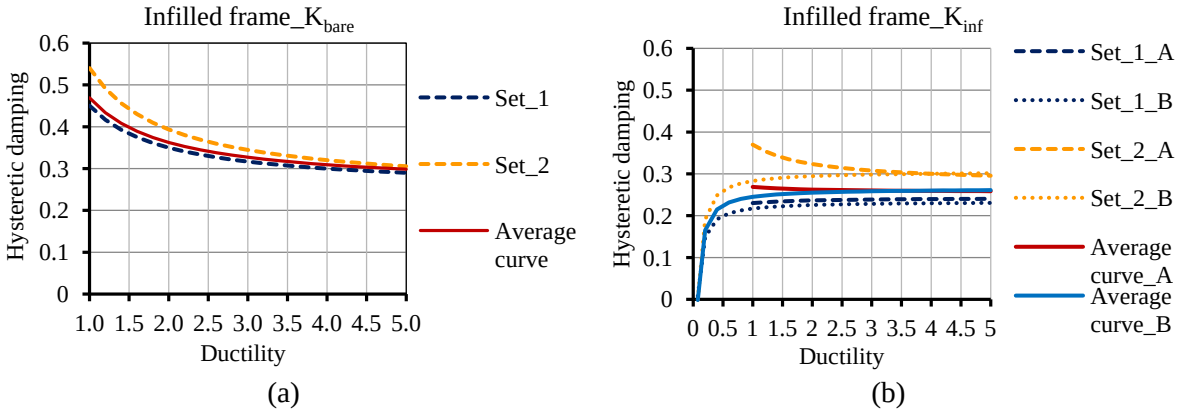

Figure 5.5. Average curves relative to the infilled frame considering the stiffness of the bare frame (a) and considering the stiffness of the infilled frame (b)

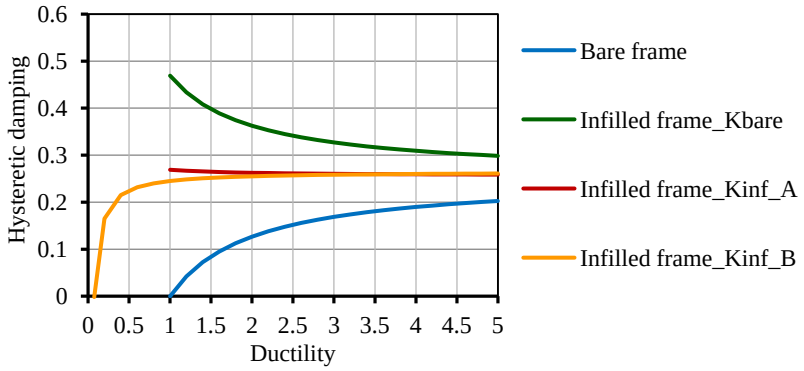

Figure 5.6. Overall average curves

6. VALIDATION OF THE PROCEDURE

In order to verify the accuracy of the procedure that was used to determine the equivalent damping of a structure, the DB assessment of a frame was carried out. The determination of the displacement demand Δ_D within the framework of DB assessment is performed through an iterative procedure. The steps are as follows:

1. Determine the effective mass m_e. For a SDOF structure this is the total mass.
2. Assume an initial value of displacement demand ($\Delta_D = \Delta_1$) .
3. Calculate the effective stiffness $K_e = K_1$ at displacement Δ_1.
4. Calculate the effective period: $T_{e1} = 2\pi\sqrt{\frac{m_e}{K_e}}$.
5. Determine the yield displacement Δ_y.
6. Determine the displacement ductility: $\mu = \frac{\Delta_D}{\Delta_y}$.
7. Calculate the effective damping $\xi_e = \xi_1$ related to the determined ductility, using the $\mu - \xi$ relationship.
8. Calculate the spectral reduction factor R_ξ corresponding to ξ_e in order to obtain the reduced displacement spectrum associated to ξ_1 for the first iteration.
9. Determine the displacement demand Δ_2 corresponding to the value of T_{e1} on the displacement spectrum relative to $\xi_1$and compare it with Δ_1.

10. If the two values are too different then the steps 3 to 9 have to be repeated starting with $\Delta_D = \Delta_2$. Proceed iteratively until the displacement determined at the step 9 is sufficiently close to that assumed.

The assessment procedure was applied to the frame 2 considered in the previous analyses: the aim was to verify that the displacement demand estimated with the iterative procedure was similar to the one obtained from the dynamic analyses. In this procedure the damping-ductility relationships obtained from the previous analyses were used; the purpose was to assess their reliability. In the assessment the average displacement spectrum relative to the accelerograms used in the dynamic analyses was adopted. The displacement spectrum was not determined by applying the reduction factor R_ξ to the ordinate of the spectrum corresponding to ξ=5% . The displacement spectrum associated to a given value of ξ was determined as average of the spectra relative to the accelerograms used in the dynamic analyses. These spectra were determined with the program SeismoSignal (SeismoSoft, 2002) for the damping values determined at step 7 of the procedure. The displacement demand calculated by the assessment procedure was then compared with the average displacement obtained by dynamic analyses. This average displacement was calculated as the average of maximum displacement resulting from each accelerogram. The accelerograms were all applied with the same scaling factor. The assessment procedure was applied to three different cases: the bare frame with the accelerograms scaled to a peak acceleration of 0.5 g, and the infilled frame with different intensities of the accelerograms, in order to obtain different values of ductility demand. With reference to the ductility-damping relationship, the bare frame was studied considering the expression given in Eqn. 5.1 while the infilled frame was studied on the basis of the Eqn. 5.3 or 5.5 depending on whether the ductility was respectively greater or less than 2. According to the above considerations, for ductility larger than 2 it was made reference to the stiffness of the bare frame, for ductility lower than 2 to the one of the infilled frame. The results of these analyses are summarized in the Table 6.1 where it is possible to compare the displacements obtained from the DB assessment with the ones obtained from dynamic analyses.

Table 6.1 Results of assessment compared to those of dynamic analyses

	Estimate from DBA procedure	Average displacement of dynamic analyses	Standard deviation	Equivalent damping
Bare frame	90 mm	100 mm	40	22%
Infilled frame $\mu>2$	122 mm	150 mm	58,6	36%
Infilled frame $\mu<2$	58 mm	40 mm	27,2	31%

7. CONCLUSIONS

The study was aimed to find a ductility-damping law that could be used in the Displacement Based assessment of existing infilled frames. This law could be very useful if applicable without knowing in detail the response of the infilled frame. In this way it could be possible to ignore the infill response, in terms of strength and stiffness, and to account for the infill only in terms of dissipation.

The procedure proposed in this study was then validated, and it could be used as reference for determining the equivalent damping of infilled frames. It is clear that, if one would generalize the results, the analyses performed for the three considered frames should be repeated for several cases and applying a large number of accelerograms,. Anyway, a possible law of general validity was also proposed.

The study allowed to obtain some conclusions about the damping of infilled frames compared to that of bare frames. As expected, the damping, which is a measure of the dissipative capacity of the structure, resulted larger for infilled frames than for bare frames. The difference between the damping of a bare and the one of an infilled frame tends to zero for high values of ductility because for these values the infilled is no longer effective; on the contrary the lower is the ductility, the greater is the increase in dissipation and therefore the damping due to the infill. In particular, for small values of ductility the damping of the infilled frame is significantly greater than that of the bare frame.

Moreover it was observed that the knowledge of the secant stiffness of the infilled frame is necessary only for very low values of ductility demand.

REFERENCES

Al-Chaar, G. (2002). Evaluating strength and stiffness of unreinforced masonry infill structures. US Army Corp of Engineers, Engineer Research and Development Center.

Cavaleri, L., Fossetti, M., and Papia, M. (2005). Infilled frames: developments in the evaluation of cyclic behaviour under lateral loads. *Structural Engineering and Mechanics*. **21:4**, 469-494.

Landi, L., Diotallevi P.P. and Tardini, A. (2012). Calibration of an equivalent strut model for the nonlinear seismic analysis of infilled RC frames. *15th World Conference on Earthquake Engineering.* Lisbon, Portugal.

Dwairi, H., Kowalsky, M.J. and Nau J.M. (2007). Equivalent Damping in Support of Direct Displacement Based Design. *Journal of Earthquake Engineering*, **11:4**, 512-530.

Iwan, W. and Gates, N. (1979). The effective period and damping of a class of hysteretic structures. *Earthquake Engineering and Structural Dynamics*, **7:3**, 199-211.

Judi, H., Fenwick, R. and Davidson, B.J., (2001). Direct displacement based design - a definition of damping. *Proceeding, NZSEE Technical Conference*. Auckland, New Zeland, paper n. 4.09

Mander, J., Priestley, M. and Park, R. (1988). Theoretical stress-strain model for confined concrete. *Journal of Structural Engineering*, ASCE **114:8**, 1804-1825.

McKenna, F. and Fenves, G. (2005). Open System for Earthquake Engineering Simulation. University of California, Berkley.

Priestley, M., Calvi, G. and Kowalsky, M. (2007). Displacement-Based Seismic Design of Structures. IUSS Press. Pavia.

SeismoSoft. Earthquake engineering software solutions. (2002). Manual and program description of the program SeismoSignal. Available from URL: http://www.seismosoft.com.